

The Work of Stone Pillars Damaged During Operation

Ievgenii Klymenko^{1*}, Iryna Grynyova², Volodymyr Pents³

¹Odessa State Academy of Civil Engineering and Architecture, Ukraine

²Odessa State Academy of Civil Engineering and Architecture, Ukraine

³Poltava National Technical Yuri Kondratyuk University, Ukraine

*Corresponding author E-mail: klimenkoew57@gmail.com

Abstract

During the experimental and statistical research the experiment was planned for the three most important factors influencing the residual load-bearing capacity of damaged stone columns rectangular cross section, namely, the depth of damage, the angle of the front damage on one of the main sections of soy and eccentricity. Numerical modeling of work of the eccentrically compressed rectangular cross section damaged during the operation of stone pillars was carried out in the LIRA-SAPR software package in a non-linear environment. The results of experimental statistical modeling made it possible to determine the influence on the throughput of each of the selected factors, as well as the mutual influence of the factors. Based on the obtained values of the destructive force for 15 column marks, in accordance with the experimental design, a three-factor experimental-statistical model of the second order was constructed. This model is adequate to the experimental error of 0.45, with 7 statistically significant factors. The analysis of the above method of calculating the damaged stone pillar in PC LIRA allows us to conclude that this method completely takes into account the actual work of the material. The difference between the calculation results and the experimental research of stone structures is within 5%.

Keywords: experimental-statistical modeling, stone pillar, damage, bearing capacity.

1. Introduction

Stone materials from ancient times, as well as the wooden materials, form the basis of construction, so the existing monuments of history and architecture, in the vast majority of them, were made of solid red brick on limestone and complex solutions.

It is known that a large part of them is located in large cities. These are historical centers of not only Ukrainian, but also European cities and separate houses and churches (Fig. 1).



Fig.1: Diocletian Palace, listed on the UNESCO list, Croatia

Modern aggressive ecology, as well as other destructive factors, worsen seriously the physical and mechanical properties of brick-work of structures of historic buildings. This suggests that brick buildings and architectural heritage buildings today are in dire need of their protection and timely restoration.

Attempts to restore architectural monuments have been already known in antiquity, but until the XVIII-XIX centuries they usually were reduced to simple repair or to restore an object with actual changes in the current history of history. As an independent discipline, the restoration of monuments originates in the middle of the XIX century. in the framework of the Christian worldview, in which "time is evaluated as a directed process with beginning and end, past and future. Therefore the possibility of irreversible loss of those values that form the fundamentals of culture, and hence the requirements for their unconditional preservation "[1, p. 32]. By this time, mostly engaged in repair, adjustment, and it was this value that was put into the very term "restoration".

2. Analysis of recent research and publications

The study of damaged during operation noncentral pressed damaged pillars of works devoted a lot of ukrainian and foreign scientists. [2 ... 7] Most of the works devoted to the consideration of issues such as determining the carrying capacity and strength elements [4, 7], the influence of various factors such as an eccentricity [6]. In Articles by Klymenko I.V. [3-5] emphasized that the current definition and forecasting of technical condition of building structures and buildings carried out intuitively and requires more detailed study. The current state building codes V.2.6-162: 2010 requires the calculation of damaged stone elements, taking into account not the linearity of deformation.

This method is the most correct, since it corresponds to the real physical model of the masonry work as a non-uniform material. During recent years, the Odessa State Academy of Civil Engineering and Architecture studies the work of noncentrally

compressed and damaged in the process of exploitation of stone structures, allowed to obtain data for further description of their stress-strain state and to develop a method for calculating residual bearing capacity [2].

3. General part

The tasks put in practice are reduced to the construction of a mathematical model that describes the whole set of parameters chosen by us and find the numerical values of these parameters. For practical description of the properties of the mathematical model of samples, methods of experimental-statistical planning were used, which allows taking into account the stochastic nature of the processes taking place in the investigated objects.

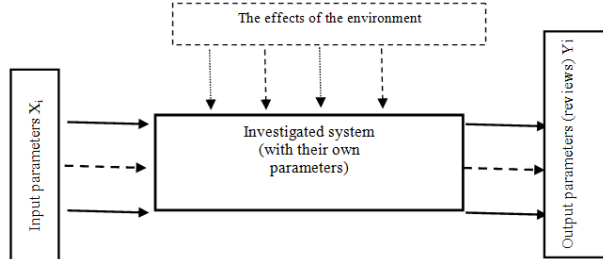


Fig. 2: Statistical model of the experiment

Given that the accepted model of the experiment is manageable, it can be schematically described using a black box model, the internal device of which is unknown, and only its inputs X_i and Y_i outputs are investigated and thus the external environment is stabilized (Fig. 2).

Analysis of scientific and technical literature and preliminary studies allowed to determine the input factors and the boundaries of their scope. The transition to the dimensionless normalized variables $-1 \leq x_i \leq +1$ is performed according to the following formula: $x_i = (X_i - X_{oi}) / \Delta X_i$ (Table 1).

Table 1: Variation of input factors

Input factors			The levels of variation			The interval of variation
Code	Value	Meas.unit	«-1»	«0»	«1»	ΔX_i
x_1	The angle of Inclination of damage θ	deg.	0	22,5	45	22,5
x_2	The depth of the damage a	mm	0	80	160	80
x_3	The relative eccentricity e_0/h	-	0	1/8	1/4	1/8

The obtained set of states of the investigated system allows us to analyze the dependence of the initial parameter of the bearing capacity of the samples on the determined factors x_1, x_2 i x_3 (Fig. 3).

Full factorial design for three factorial experiment has 27 lines - state of the object, which is excessive for the task, therefore, for the practical optimization of the accepted experimental model, a 15-point symmetric plan was adopted. With this approach, as a result of the experiment, we will receive a statistically reliable result with a minimum number of investigated samples.

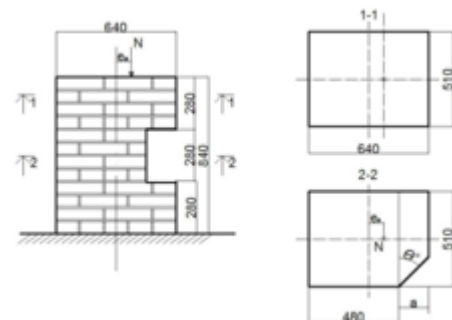


Fig. 3: Scheme for modeling of damaged sample-pillar

The formed matrix of the experiment with Physical variables of variation of the investigated parameters for a three-factor quadratic ES-model has the form (Table 2)

Table 2: Physical variables of the studied parameters

№ experiment	The coded values of factors			Actual factors		
	x_1	x_2	x_3	The angle of inclination of damage θ , deg.	The depth of the damage a , mm	The relative eccentricity e_0/h
1	-1	-1	-1	0	0	0
2	-1	1	-1	0	320	0
3	0	0	-1	22,5	160	0
4	1	-1	-1	45	0	0
5	1	1	-1	45	320	0
6	-1	0	0	0	160	1/8
7	0	-1	0	22,5	0	1/8
8	0	0	0	22,5	160	1/8
9	0	1	0	22,5	320	1/8
10	1	0	0	45	160	1/8
11	-1	-1	1	0	0	1/4
12	-1	1	1	0	320	1/4
13	0	0	1	22,5	160	1/4
14	1	-1	1	45	0	1/4
15	1	1	1	45	320	1/4

Tests of the samples started with a control load of forces equal to 1/6 of the destructive load. During the control loading devices mounted on opposite sides symmetrically with respect to the sample plane it should show the same strain. Otherwise, the sample was unloaded, moved in the desired direction, and again controlled crimping. The results of the indicator counts did not differ by more than 15%. When the same indications of symmetrical devices were reached, the load shedding was carried out not to zero, but to about 100 kgs to ensure the traverse contacts the press with the sample. The load was applied in steps of 1/10 ... 1/16 of the expected breaking force with an exposure of 5-6 minutes at each load stage. The rate of stress growth (6 ... 4) kgf / cm² per second.

Before and after the countdown on the instruments, they were recorded at each stage of loading.

During the loading process, the deflection from the load was measured, which was fed stepwise, as well as the appearance of cracks and their opening. The fig.4 shows the destruction of the prototype pillar -1 -1 -1 with central compression. With a longitudinal external force equal to $N = 50$ tf, at the loading level ($N/N_u = 0,71$), the main cracks appeared, which opened with increasing load. The nature of the cracks, the angle of inclination and their location are normal and expected. The destruction occurred after the load was held at $N = 70,035$ tf, with subsequent loading, small longitudinal cracks appeared to open and the structure ceased to take on any further load.

With the magnitude of the eccentricity of the applied load (up to 160 mm) and the depth of the damage (up to 320 mm), the bearing capacity of the damaged pillars is reduced, as shown in Fig. 6 when the load of the column 1 1 + 1 is loaded at a total $N = 6.67$ tf, which was $N/N_u = 0,71$ from the devastating load. During the

endurance of the load, the main longitudinal cracks followed, and the layering of the structural element under the applied load began to occur. The final destruction of the structure and the failure to perceive the loads occurred after the shutdown and subsequent loading to $N = 9.338$ tf.



Fig. 4: Testing of a prototype of a pillar C -1 -1 -1 and a twin sample C 1 -1 -1 with a central compression

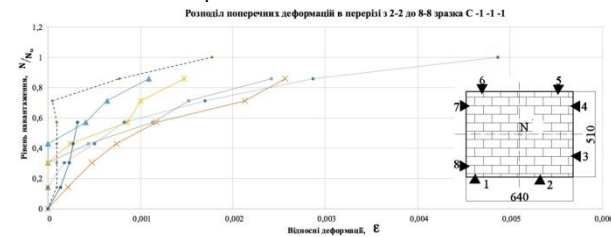


Fig. 5: Deformations in the masonry of the pillar C -1 -1 -1 and the twin sample C 1 -1 -1

With the magnitude of the eccentricity of the applied load (up to 160 mm) and the depth of the damage (up to 320 mm), the bearing capacity of the damaged pillars is reduced, as shown in Fig. 6 when the load of the column 1 1 + 1 is loaded at a total $N = 6.67$ tf, which was $N/N_u = 0,71$ from the devastating load. During the endurance of the load, the main longitudinal cracks followed, and the layering of the structural element under the applied load began to occur. The final destruction of the structure and the failure to perceive the loads occurred after the shutdown and subsequent loading to $N = 9.338$ tf.



Fig. 6: Testing of the prototype of the column C 1 1 1

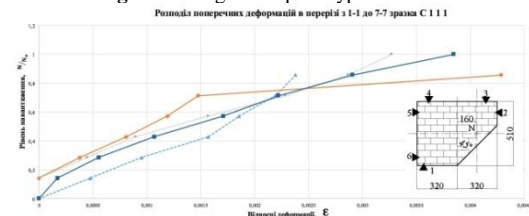


Fig.7: Deformations in the masonry of C 1 1 1

As seen in Fig. 7 with the test of the sample 1 0 0, large stresses occur at the boundary with the sensors 6, 7, 8 from the load applied with the eccentricity. In the region of the sensor fixation, longitudinal cracks became characteristic and indicative, wide open. Also, in the sample, a change in the "sign" was observed before the value of the arising deformations. The entire design undergoes compression, but because of the displacement of the eccentricity, the facet with the 3,4 sensors works by stretching. This phenomenon is explained by the fact that the structure is bent

under pressure, but as the stone structures do not work well, a break occurs soon. Destruction occurs at $N = 30,682$ tf.



Fig. 8: Testing of the prototype of the column C 1 0 0



Fig. 9: Deformations in the masonry of the C 1 0 0

Table 3: Summary data of destructive loads in relation to damage

Code	Sketch	Destructive load, tf	Code	Sketch	Destructive load, tf
1	2	3	4	5	6
C -1 -1 -1		70,035	C -1 -1 -1		2
C 0 0 -1		45,356	C 1 -1 -1		70,035
C 1 1 -1		45,356	C -1 0 0		34
C 0 -1 0		76,71	C 0 0 0		46,69
C 0 1 0		44,689	C 1 0 0		30,682
C -1 -1 1		56,695	C -1 1 1		1,334

C 0 0 1		46,023	C 1 - 1 1		56,695
C 1 1 1		9,338			

Based on the received values of the destructive force (R_u , tf) for the 15 variations of the pillars, according to the experimental plan, a 3-factor experimental-statistical model (ES-model) of the 2nd order (1) was constructed. The ES model is adequate for an experiment with the error $s_e[\ln\{R_u\}] = 0.45$, with 7 statistically significant coefficients.

$$\ln\{R_u\} = 4.075 + 0.497x_1 - 0.634x_1x_2 \pm 0x_1x_3 + 0.721x_1^2 - 1.008x_2 \pm 0x_2^2 \pm 0x_2x_3 - 0.239x_3 - 0.374x_3^2 \quad (1)$$

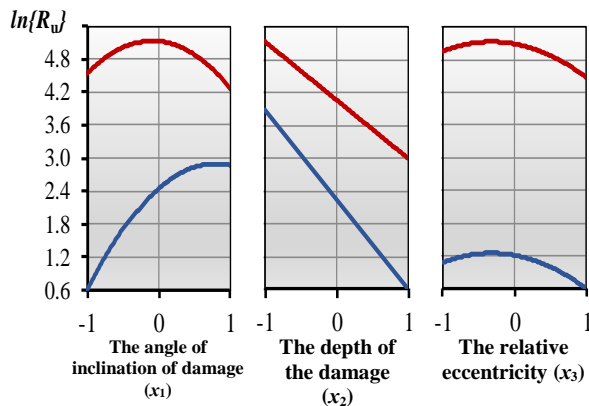


Fig. 10: One-factor dependences of influence of variation of input factors on destructive loading

The main general indicators of the model in the coordinates extremes for R_u include a minimum $R_{u,min} = 1,8$ tf (for $x_1=-1, x_2=x_3=+1$) and maximum $R_{u,max} = 168,7$ tf (for $x_1=-0.095, x_2=-1, x_3=-0.320$) levels; absolute $\Delta\{R_u\} = 166.9$ tf and relative $\delta\{R_u\} = 93.7$ times.

Estimates of the coefficients of the model and generalizing indicators characterize the individual and combined effects of the angle of inclination of the damage front (θ , degrees), the depth of damage (a , mm), and the relative eccentricity (e_0/h) of the cutoff on the level of destructive force. Visualization of this effect is presented on Fig. 3 and 4

According from the estimations of the ES-model and single-factor local fields (Fig. 10), the significant influence on R_u makes X_2 with the increase of the depth of damage in the section of the column significantly decreases the destructive load, so in the zone of maximum values of 8.5 times.

From the analysis of the model it follows: the limiting load of sample pillars depends on the magnitude of the angle of inclination of the front of the damage x_1 , and on the relative eccentricity x_3 . So, with an increase in the eccentricity e_0/h (assuming $x_1=-1$) of the applied load, R_u first grows by about 18% for $x_3=-0.40$, and then decreases by about 47% for $x_3=+1$. Influence of the angle of inclination of the front of the damage (provided $x_3=-1$) on the external load is slightly larger. With the change of X_1 from 0 to

$22.5^\circ R_u$ increases by 79%, and with further change of X_1 from 22.5° to 45° , the destructive load decreases more than 2 times (from 140.9 to 59.7 tf).

The analysis of the presented diagram (Fig. 11) constructed on the three-factor model (2) shows that the pillars can withstand the maximum load in $R_u=167.1$ tf, but only if the angle of inclination of the front of the damage (X_1) is about $18-22.5^\circ$, and the relative eccentricity (X_3) will be about $1/8$ of the applied load.

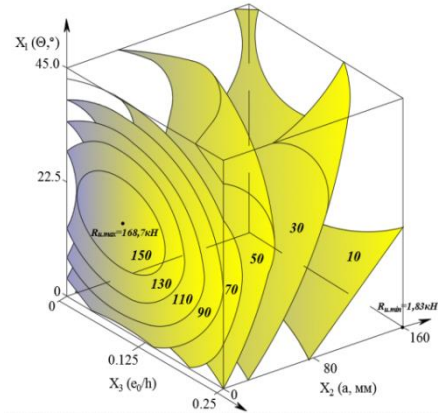


Fig. 11: Influence X_1-X_3 on the destructive loading of the pillars

3.1. Modeling in PC LIRA

According to the current norms, on the proposal of L. I. Onishchik diagram of "stress-deformation" for the masonry has the following form (Figure 12):

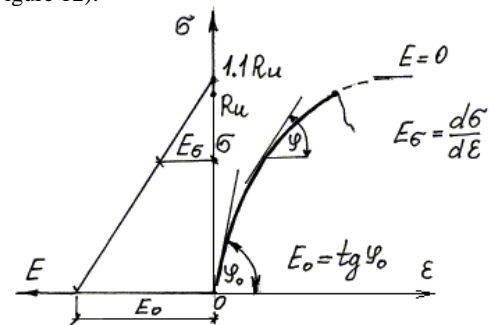


Fig. 12: The deformation pattern of the masonry

To construct the dependence curve "ε - σ" for this masonry, we use the preconditions for calculating from the textbook Vakhnenko P.F.

$$\epsilon = \frac{\sigma_1}{E_0 \cdot \left(1 - \frac{\sigma_1}{1.1 \cdot R_u}\right)} \quad (1)$$

where:

E_0 - initial modulus of masonry deformation (modulus of elasticity at stressed, close to zero)

R_u - average compressive strength

The initial modulus E_0 of elasticity can be expressed through the ultimate strength:

$$E_0 = \alpha \cdot R_u \quad (2)$$

where

α - elastic characteristics of the masonry, which depends on the type of masonry and brand of the solution

The strength of a masonry, studied in this work is theoretically determined by the formula of L.I. Onishchik:

$$R_u = AR_1 \left(1 - \frac{a}{b + R_2/2R_1}\right) \gamma, \quad (3)$$

where:

- R_1 - the compressive strength of the stone;
- R_2 - strength of the solution (cubic strength);
- A - coefficient that characterizes the maximum possible strength of the masonry and is determined by the formula:

$$A = \frac{100 + R_1}{100m + nR_1}$$

γ -coefficient that is used in determining the strength of masonry on different solutions of low grades (M25 and below)

In this case, the brand M25: $= 11.1 \text{ MPa}$; $= 5.52 \text{ MPa}$; $a = 0.2$; $b = 0.3$; $m = 1.25$; $n = 3$ (Table 2 [75]); $A = 0.46$; $\gamma = 1$ substituting in the formula (3)

$$R_u = 0,46 \cdot 11,1 \cdot \left(1 - \frac{0,2}{0,3 + 5,52/2 \cdot 11,1} \right) \cdot 1 = 3,24 \text{ МПа} \quad (5)$$

To solve the problem, it is necessary to construct a graph of the dependence of " $\epsilon - \sigma$ " by substituting the coordinates into formula 3 (Tab. 4). Using the Microsoft Excel software program, the resulting characteristic points are presented as a graph.

Table 4 : The dependence of " $\epsilon - \sigma$ " by substituting the coordinates into formula 3

R_u	E_0	σ	ϵ
3,24	3800	0	0
		0.5	0.000153
		1	0.000366
		1.5	0.000682
		2	0.001201
		2.5	0.00221
		3	0.005019
3.24	0.009486		

The resulting calculation results are presented in Fig. 13

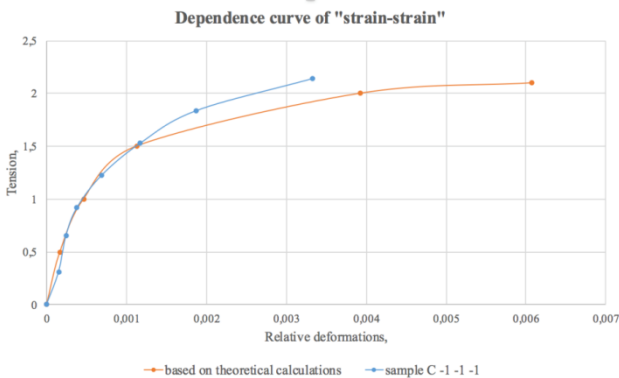


Fig. 13: Graph of tension and deformation

The method of evaluation of residual bearing capacity in the software complex, non-destructive method is proposed hereafter. At the first stage, we create points on coordinates, which later connect and set the boundary conditions to nodes in five degrees of freedom. At the second stage, we set the stiffness of the elements. Using the "Hardness \rightarrow Hardness Elements" menu, we call the "Elemental Hardness" dialog. In this window, click on the "Add" button to display the list. Choose the third dialog "Plastic, Volume, Numerical", the type of section - "Volume Limit Elements", and then put a tick on the account of nonlinearity and press "parameters of the material", choose the "law of nonlinear deformation", in our case, it is 14 (piecewise -linear law of deformation), and then we introduce data on the characteristics of the material from the received graph of the dependence of "stress-deformation" (Fig. 13)

The pillar was divided into finite elements in the form of rectangular parallelepipeds with a face dimension of 1 to 2 cm, as well as octal and six-node endpoints in the form of triangular and quadrangular prisms in places where this required the geometry of the

sample for modeling the slope of the shelves and the front of the damage.

The laying was given by physically nonlinear spatial eight-node and six-node isoparametric KEs of type 236 - "physically nonlinear universal spatial 8-node isoperimetric Limit Elements " (Fig. 14) and a metal plate for the transfer of load 234, taking into account geometric and physical nonlinearity.

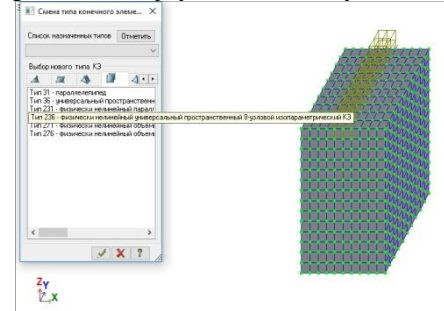


Fig. 14: Selecting the type of the final element

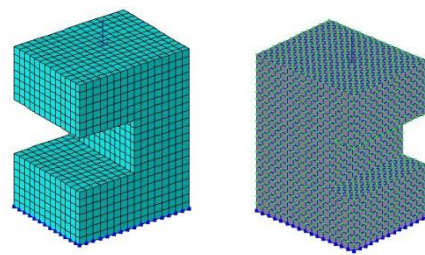


Fig. 15: Finite Element Model of a Damaged Column

The resulting model is close to a full-scale experiment (Fig.15,16,17). We perform the calculation of the model, and the results are obtained in tabular form.

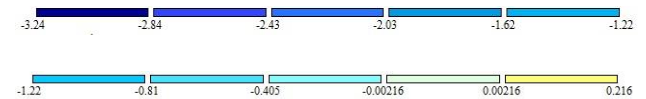


Fig.16: Isolation of normal voltages in t / m2

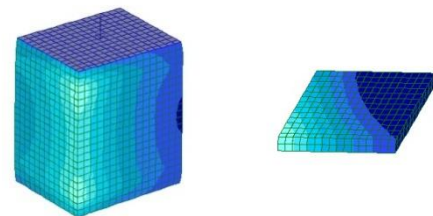


Fig. 17: Isolation stresses in the C -1-1-1 column

Figures 16,17 show that in the case of small areas of damage, the protective layer of concrete is less, compressing stresses are approximately the same throughout the section under consideration. In the case when the rebars of concrete exposed the reinforcing bars, a redistribution of compressive stresses on the reinforcement is observed, which provides additional strength of the damaged columns during compression.

In all the specimens examined, the neutral line in the damaged section is beyond its limits and has the form close to the straight line. It is parallel to the damage front in the case of its parallelism of one of the main axes of the section. In the case of "skew" damage, the turn of the neutral line occurs relative to the main axes of the section and the front of the damage.

4. Conclusions

According to the experimental-statistical model and single-factor local fields, the greatest influence on the bearing capacity gives

the damage depth at the intersection of the pillar. The analysis of the above method of calculating the damaged stone pillar in PC LIRA allows us to conclude that this method completely takes into account the actual work of the material. The difference between the calculation results and the experimental research of stone structures is within 5%.

References

- [1] DSTU-N BV. 1.2-18: 2016. "Guidelines for the inspection of buildings and structures for the determination and evaluation of their technical condition" Minrehionbud Ukrayiny. – K., 2017. -pp 45
- [2] Grynyova I.I., "Methods of experimental study of stress-strain state damaged stone pillar", Bulletin of the Odessa State Academy of Civil Engineering and Architecture, Vol. 67 (2017), pp. 20-26
- [3] Klymenko I.V., Shepitko S.A., "Estimation of technical condition of stone buildings and structures" Bulletin of the Odessa State Academy of Civil Engineering and Architecture, Vol. 67 (2017), pp. 20-26
- [4] Klymenko I.V., Shapoval S.L., "Experimental studies of masonry at its local compression: Sb. "Sectoral engineering, construction" PDTU im. Yuriya Kondratyuka, Vol.7.,(2001), pp. 58-64
- [5] Klymenko I.V., "Technical problems of managing the residual resource of objects of cultural heritage" Zberezheniya istorichnoyi zabudovy tsentra Odesy shlyakhom vklyuchennya do osnovnoho spysku vsesvitn'oyi spadshchyny YUNESKO: Materialy III i IV konferentsiy, (2016) pp. 68-74
- [6] Baklushev E.V., "Influence of flexibility and eccentricity of load application on reliability of eccentrically compressed elements" , Beton i zhelezobeton, Vol.4, (1992) pp. 16-17
- [7] Pohribnyi V, Dovzhenko O, Karabash L, Usenko I, The design of concrete elements strength under local compression based on the variational method in the plasticity theory, Web of Conferences, (2017) Vol. 116, <https://doi.org/10.1051/mateconf/20171160201>
- [8] Kochkarev, D., & Galinska, T. (2017). Calculation methodology of reinforced concrete elements based on calculated resistance of reinforced concrete. Paper presented at the MATEC Web of Conferences, , 116 <https://doi.org/10.1051/mateconf/201711602020>
- [9] Piskunov, V. G., Goryk, A. V., & Cherednikov, V. N. (2000). Modeling of transverse shears of piecewise homogeneous composite bars using an iterative process with account of tangential loads. 1. construction of a model. *Mechanics of Composite Materials*, 36(4), 287-296. <https://doi.org/10.1007/BF02262807>